Level Crossing Rate and Average Fade Duration in $\mathcal{F}$ Composite Fading Channels

Seong Ki Yoo, *Member, IEEE,* Simon L. Cotton, *Senior Member, IEEE,* Paschalis C. Sofotasios, *Senior Member, IEEE,* Sami Muhaidat, *Senior Member, IEEE,* and George K. Karagiannidis, *Fellow, IEEE*

***Abstract*—In this paper, we derive exact closed-form expressions for the level crossing rate (LCR) and average fade duration (AFD) of the signal envelope in $\mathcal{F}$ composite fading channels. Using the novel expressions, we then investigate the behavior of the LCR and AFD for different multipath fading and shadowing conditions. It is shown that multipath fading has a more significant effect on the LCR at lower fade levels while shadowing tends to have a discernible impact on higher threshold levels. In contrast, shadowing has a more noticeable effect on the AFD compared to multipath fading at both lower and higher levels. Approximate expressions for the LCR and AFD are also provided, and shown to be in good agreement with the exact LCR and AFD as they approach lower and higher threshold levels. The offered results are expected to be useful in the design of emerging systems such as device-to-device communications.**

***Index Terms*—Average fade duration, composite fading, Fisher-Snedecor $\mathcal{F}$ distribution and level crossing rate.**

I. Introduction

COMPOSITE fading models have seen a resurgence in popularity over the last few years, driven in part by the complex nature of many emergent wireless applications which can undergo simultaneous multipath fading and shadowing [1], [2]. These models are highly beneficial in the characterization of fading channels as they circumvent the requirement to determine an appropriate smoothing window size for the computation of the local mean signal. It is widely known that this procedure can affect the parameter estimation process and subsequently any inferences made from experimental data.

Recently, the Fisher-Snedecor $\mathcal{F}$ distribution has been proposed to model a Nakagami-m fading envelope in which the root-mean-square (RMS) power is subject to variations induced by an inverse Nakagami-m random variable [3]. In the same contribution, it was shown that the $\mathcal{F}$ composite fading model offers a number of potential advantages over many of the existing composite fading models commonly used in the literature. Two noted prominent features were the enhanced fit to physical measurement data relating to device-to-device scenarios and the mathematical simplicity of its fundamental statistical metrics and performance measures. Following from this, the authors of [4] introduced a slight modification to the underlying inverse Nakagami-m PDF from that used in [3] to ensure stability in the ensuing performance analysis.

While first-order statistics, such as the probability density function (PDF) and cumulative distribution function (CDF), are useful for interpreting the overall distribution of fades in fading channels, unfortunately they provide no indication of how these fades are distributed with respect to time. On the contrary, second-order statistics, such as the level crossing rate (LCR) and the average fade duration (AFD), do convey this information. Since the LCR and AFD provide a direct indication of the rate of change of the signal with respect to time, they are useful in the design of communication systems and analysis of their performance [5]. Additionally, in ultra-reliable low latency communication (uRLLC), which is one of three main use cases for 5G networks and beyond [6], it is important to accurately characterize the frequency of outage and average outage duration of wireless links, which reflect a *delay* in the end-to-end communication process.

Driven by the need to develop a fuller understanding of composite fading channels, a number of studies have investigated their first-order statistics characteristics [2], [7]. For example, in [2], the key statistics of the κ-μ / inverse gamma and η-μ / inverse gamma composite fading models were developed and then utilized to characterize the composite fading channels observed in wearable, device-to-device and vehicular-to-vehicular (V2V) channels. In contrast, comparatively few results on the second-order statistics of composite fading channels are available in the literature [8–10]. Moreover, for the majority of cases, closed-form expressions for the LCR and AFD are not available and thus the solutions which do exist are often not convenient to work with. Additionally, many of these second-order statistics deal with so-called line-of-sight (LOS) composite fading channels. However, these models are not able to account for conventional large-scale effects, i.e., shadowing of the RMS power.

Motivated by these factors, in this paper, exact closed-form expressions for the LCR and AFD of the signal envelope in $\mathcal{F}$ composite fading channels are derived. As a byproduct of our analysis, we also obtain an expression for the joint PDF of an inverse Nakagami-m random process and its time derivative. To the best of our knowledge, all of these expressions are new, and have not been previously reported in open technical literature. Using the newly obtained expressions, we analyze the behavior of the LCR and AFD over $\mathcal{F}$ composite fading channels for different multipath fading and shadowing

This work was supported in part by the U.K. Engineering and Physical Sciences Research Council under Grant No. EP/L026074/1, by the Department for the Economy Northern Ireland through Grant No. USI080 and by Khalifa University under Grant No. KU/RC1-C2PS-T2/8474000137 and Grant No. KU/FSU-8474000122.

S. K. Yoo and S. L. Cotton are with Centre for Wireless Innovation, ECIT Institute, Queen's University Belfast, Belfast BT3 9DT, U.K. (e-mail: {sk.yoo; simon.cotton}@qub.ac.uk)

P. C. Sofotasios is with the Center for Cyber-Physical Systems, Department of Electrical and Computer Engineering, Khalifa University, Abu Dhabi 127788, UAE, and also with the Department of Electrical Engineering, Tampere University, Tampere 33101, Finland (e-mail: p.sofotasios@ieee.org)

S. Muhaidat is with the Center for Cyber-Physical Systems, Department of Electrical and Computer Engineering, Khalifa University, Abu Dhabi 127788, UAE (e-mail: muhaidat@ieee.org)

G. K. Karagiannidis is with the Department of Electrical & Computer Engineering, Aristotle University of Thessaloniki, Thessaloniki 54124, Greece (e-mail: geokarag@auth.gr)

conditions as well as demonstrating their generality through reduction to a number of special cases.

II. The $\mathcal{F}$ Composite Fading Model

The received signal envelope in an $\mathcal{F}$ composite fading channel can be interpreted as the product of two independent random processes, i.e., $R = XY$, where X is a Nakagami-m random variable with the shape parameter m and spread parameter $\Omega = \mathbb{E}[X^2]$, with $\mathbb{E}[\cdot]$ denoting statistical expectation, whose PDF is given by

$$f_X(x) = \frac{2m^m x^{2m-1}}{\Gamma(m)\,\Omega^m} \exp\left(-\frac{mx^2}{\Omega}\right) \tag{1}$$

where $\Gamma[\cdot]$ represents the gamma function [11, eq. (8.310.1)]. Then, Y is a normalized inverse Nakagami-m random variable where m_s is the shape parameter and $\mathbb{E}[Y^2] = 1$, such that

$$f_Y(y) = \frac{2(m_s-1)^{m_s}}{\Gamma(m_s)\,y^{2m_s+1}} \exp\left(-\frac{(m_s-1)}{y^2}\right). \tag{2}$$

Consequently, the resultant PDF of the received signal envelope in an $\mathcal{F}$ composite fading channel can be obtained through the relation [12], $f_R(r) = \int_{-\infty}^{\infty} \frac{1}{|y|} f_{XY}\left(\frac{r}{y}, y\right) \mathrm{d}y$, where $f_{XY}(x,y)$ represents the joint PDF of the processes $f_X(x)$ and $f_Y(y)$. Since the Nakagami-m random variable, X, and the normalized inverse Nakagami-m random variable, Y, are statistically independent, i.e., $f_{XY}(x,y) = f_X(x) f_Y(y)$, it follows that $f_R(r) = \int_{-\infty}^{\infty} \frac{1}{|y|} f_X\left(\frac{r}{y}\right) f_Y(y)\,\mathrm{d}y$. By substituting (1) and (2) into this equation, performing a simple transformation of variables and using [11, eq. (3.326.2)] along with some algebraic manipulations, we arrive at the same expression as that given in [4, eq. (5)], namely

$$f_R(r) = \frac{2m^m (m_s-1)^{m_s} \Omega^{m_s} r^{2m-1}}{B(m,m_s)\left(mr^2 + (m_s-1)\Omega\right)^{m+m_s}},\ m_s > 1 \tag{3}$$

where $B(\cdot,\cdot)$ denotes the beta function [11, eq. (8.384.1)]. In this model, m and $\Omega = \mathbb{E}[R^2]$ represent the multipath fading severity and mean signal power, respectively. Additionally, m_s denotes the shadowing severity parameter which controls the amount of the shadowing of the RMS signal power.

Although the corresponding moment generating function (MGF) presented in [3, eq. (10)] and [4, eq. (10)] was obtained using the standard statistical procedure, we make the point that it cannot be referred to as a true MGF as it cannot be guaranteed that the moments are finite over the entire space of m_s parameter. Nonetheless, the expression appears stable and useful as a substitution for evaluating many of the performance measures associated with $\mathcal{F}$ composite fading channels.

III. Second - Order Statistics

A. Level Crossing Rate

1) Exact Results: The LCR, $N_R(r)$, is defined as the rate at which the signal envelope crosses a given threshold level r in a positive (or in a negative) direction per unit time. This is obtained as

$$N_R(r) = \int_0^{\infty} \dot{r}\, f_{R,\,\dot{R}}(r,\dot{r})\,\mathrm{d}\dot{r} \tag{4}$$

where $\dot{r}$ denotes the time derivative of r. In (4), the joint PDF of R and $\dot{R}$ can be obtained in a double integral form as [13]

$$f_{R,\dot{R}}(r,\dot{r}) = \int_0^{\infty}\int_{-\infty}^{\infty} \frac{1}{y^2} f_{X,\dot{X}}\left(\frac{r}{y}, \frac{\dot{r}}{y} - \frac{r\dot{y}}{y^2}\right) f_{Y,\dot{Y}}(y,\dot{y})\,\mathrm{d}\dot{y}\,\mathrm{d}y \tag{5}$$

where $\dot{X}$ and $\dot{Y}$ denote the time derivative of X and Y, respectively. It has been shown in [14] that a Nakagami-m random process, X, and its time derivative, $\dot{X}$, are mutually independent, i.e., $f_{X,\dot{X}}\left(\frac{r}{y}, \frac{\dot{r}}{y} - \frac{r\dot{y}}{y^2}\right) = f_X\left(\frac{r}{y}\right) f_{\dot{X}}\left(\frac{\dot{r}}{y} - \frac{r\dot{y}}{y^2}\right)$. Moreover, the time derivative, $\dot{X}$, follows a zero-mean Gaussian PDF with variance $\dot{\sigma}_X^2 = \pi^2 f_m^2 \Omega/m$ where f_m is the maximum Doppler frequency, such that

$$f_{\dot{X}}\left(\frac{\dot{r}}{y} - \frac{r\dot{y}}{y^2}\right) = \frac{1}{\sqrt{2\pi}\dot{\sigma}_X} \exp\left[-\frac{\left((\dot{r}y - r\dot{y})/y^2\right)^2}{2\dot{\sigma}_X^2}\right]. \tag{6}$$

Hence, with the aid of (1) and (6), the joint PDF of X and $\dot{X}$ in (5) can be obtained as

$$\begin{aligned} f_{X,\dot{X}}\left(\frac{r}{y}, \frac{\dot{r}}{y} - \frac{r\dot{y}}{y^2}\right) =& \frac{2m^m}{\Gamma(m)\,\Omega^m \sqrt{2\pi}\dot{\sigma}_X} \left(\frac{r}{y}\right)^{2m-1} \\ &\times \exp\left(-\frac{mr^2}{\Omega y^2}\right) \exp\left[-\frac{\left((\dot{r}y - r\dot{y})/y^2\right)^2}{2\dot{\sigma}_X^2}\right]. \end{aligned} \tag{7}$$

Using the simple relationship which exists between a Nakagami-m process and an inverse Nakagami-m process, we can write $Y = 1/Z$ where Z is a normalized Nakagami-m process with shape parameter m_s and spread parameter $\mathbb{E}[Z^2]$ = 1 such that its PDF is given by

$$f_Z(z) = \frac{2(m_s-1)^{m_s} z^{2m_s-1}}{\Gamma(m_s)} \exp\left(-(m_s-1)z^2\right). \tag{8}$$

Similarly, it is worth remarking that a normalized Nakagami-m random process, Z, and its time derivative, $\dot{Z}$, are independent and the time derivative, $\dot{Z}$, follows zero-mean Gaussian PDF with variance $\dot{\sigma}_Z^2 = (\pi f_m)^2/(m_s-1)$.

To obtain the joint PDF of Y and $\dot{Y}$, we need to find the time derivative of both sides of $Y = 1/Z$, i.e., $\dot{Y} = -\dot{Z}/Z^2 = -Y^2\dot{Z}$. For fixed $Y = y$, it can be shown that the time derivative, $\dot{Y}$, also follows a zero-mean Gaussian PDF with the conditional variance $\sigma_{\dot{Y}|Y}^2 = y^4\dot{\sigma}_Z^2$. Consequently, the conditional PDF, $f_{Y|\dot{Y}}(y|\dot{y})$, can be readily expressed as

$$f_{Y|\dot{Y}}(y|\dot{y}) = \frac{1}{\sqrt{2\pi}\dot{\sigma}_Z y^2} \exp\left[-\frac{\dot{y}^2}{2\dot{\sigma}_Z^2 y^4}\right]. \tag{9}$$

Using $f_{Y,\dot{Y}}(y,\dot{y}) = f_{Y|\dot{Y}}(y|\dot{y})\, f_Y(y)$ with the aid of (2) and (9), we can then obtain the joint PDF of Y and $\dot{Y}$ as follows

$$f_{Y,\dot{Y}}(y,\dot{y}) = \frac{2(m_s-1)^{m_s} \exp\left(-\frac{\dot{y}^2}{2\dot{\sigma}_Z^2 y^4} - \frac{(m_s-1)}{y^2}\right)}{\sqrt{2\pi}\dot{\sigma}_Z \Gamma(m_s)\, y^{2m_s+3}}. \tag{10}$$

From (10) it becomes apparent that an inverse Nakagami-m random process and its time derivative are not independent.

Substituting (7) and (10) into (5), the joint PDF of R and $\dot{R}$ can be obtained in (11) at the top of the next page. By carrying out some algebraic manipulations using [11, eq. (3.323.2)] and [11, eq. (3.381.4)], (11) can be expressed in closed-form as given in (12) at the top of the next page. Now, substituting (12) into (4) and using [11, eq. (3.241.4)] along with some algebraic manipulations, the LCR of the signal envelope in $\mathcal{F}$

$$f_{R,\dot{R}}(r,\dot{r}) = \int_0^{\infty}\int_{-\infty}^{\infty} \frac{4m^m (m_s-1)^{m_s} r^{2m-1}}{2\pi\Gamma(m)\Gamma(m_s)\,\Omega^m \dot{\sigma}_X \dot{\sigma}_Z y^{2m+2m_s+4}} \exp\left[-\frac{mr^2}{\Omega y^2} - \frac{(m_s-1)}{y^2} - \frac{\left((\dot{r}y - r\dot{y})/y^2\right)^2}{2\dot{\sigma}_X^2} - \frac{\dot{y}^2}{2\dot{\sigma}_Z^2 y^4}\right] \mathrm{d}\dot{y}\,\mathrm{d}y \quad (11)$$

$$f_{R,\dot{R}}(r,\dot{r}) = \frac{2m^m (m_s-1)^{m_s} r^{2m-1}\Gamma\left(m+m_s+\frac{1}{2}\right)}{\sqrt{2\pi}\,\Omega^m \Gamma(m)\,\Gamma(m_s)\,\sqrt{r^2\dot{\sigma}_Z^2+\dot{\sigma}_X^2}} \left(\frac{mr^2}{\Omega} + (m_s-1) + \frac{\dot{r}^2}{2\left(r^2\dot{\sigma}_Z^2+\dot{\sigma}_X^2\right)}\right)^{-m-m_s-\frac{1}{2}} \quad (12)$$

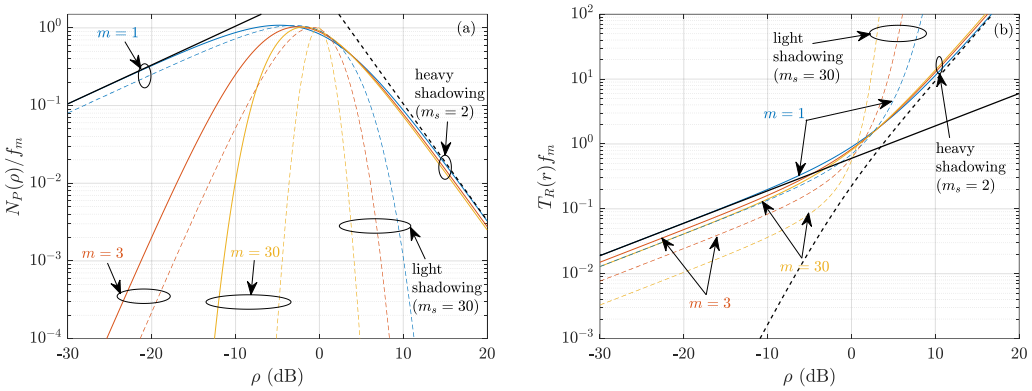

Fig. 1. Normalized (a) LCRs and (b) AFDs over $\mathcal{F}$ composite fading channels considering different conditions of the multipath fading and shadowing. The approximate LCRs and AFDs for lower ρ (black continuous lines) and higher ρ (black dash lines) levels are also present for the case of $m = 1$ and $m_s = 2$.

composite fading channels can be expressed as

$$\frac{N_R(r)}{f_m} = \frac{\sqrt{2\pi}\Gamma\left(m+m_s-\frac{1}{2}\right) m^{m-\frac{1}{2}} [(m_s-1)\Omega]^{m_s-\frac{1}{2}} r^{2m-1}}{\Gamma(m)\,\Gamma(m_s)\,[mr^2+(m_s-1)\,\Omega]^{m+m_s-1}}. \quad (13)$$

By also considering the normalized signal envelope ($P = R/\sqrt{\Omega}$), (13) can be re-written as follows

$$\frac{N_P(\rho)}{f_m} = \frac{\sqrt{2\pi}\Gamma\left(m+m_s-\frac{1}{2}\right)(m_s-1)^{m_s-\frac{1}{2}} m^{m-\frac{1}{2}} \rho^{2m-1}}{\Gamma(m)\,\Gamma(m_s)\,[(m_s-1)+m\rho^2]^{m+m_s-1}}. \quad (14)$$

2) Special Cases: While the closed-form expressions given in (13) and (14) are convenient to handle both analytically and numerically, even greater insights into the role of the involved parameters can obtained by observing what happens when threshold levels begin to approach extreme values. To this end, when $m\rho^2 \gg m_s - 1$, then $m_s - 1 + m\rho^2 \simeq m\rho^2$, yielding

$$\frac{N_P(\rho)}{f_m} \simeq \frac{\sqrt{2\pi}\,\Gamma\left(m+m_s-\frac{1}{2}\right)(m_s-1)^{m_s-\frac{1}{2}}}{\Gamma(m)\Gamma(m_s) m^{m_s-\frac{1}{2}} \rho^{2m_s-1}}. \quad (15)$$

Likewise, for the case that $m\rho^2 \ll m_s - 1$, it follows that $m_s - 1 + m\rho^2 \simeq m_s - 1$, which after some manipulations yields

$$\frac{N_P(\rho)}{f_m} \simeq \frac{\sqrt{2\pi}\,\Gamma\left(m+m_s-\frac{1}{2}\right) m^m \rho^{2m-1}}{\Gamma(m)\Gamma(m_s)(m_s-1)^m}. \quad (16)$$

B. Average Fade Duration

1) Exact Results: The AFD, $T_R(r)$, is defined as the average length of time during which the signal envelope remains below a given threshold level. This is represented mathematically as $T_R(r) \triangleq F_R(r)/N_R(r)$, where $F_R(r)$ represents the CDF of the $\mathcal{F}$ composite fading signal envelope as given in [4, eq. (12)]. Thus, by substituting [4, eq. (12)] and (13) into the above expression, it readily follows that

$$T_R(r) f_m = \frac{\Gamma(m+m_s)\left[mr^2+(m_s-1)\,\Omega\right]^{m+m_s-1}}{\Gamma\left(m+m_s-\frac{1}{2}\right)\,(m_s-1)^{m+m_s-\frac{1}{2}}\Omega^{m+m_s}} \times \frac{r\sqrt{\Omega}}{\sqrt{2m\,\pi}}\,{}_2F_1\left(m+m_s, m; 1+m; -\frac{mr^2}{(m_s-1)\Omega}\right) \quad (17)$$

where ${}_2F_1(\cdot,\cdot;\cdot;\cdot)$ denotes the Gauss hypergeometric function [11, eq. (9.111)]. Similarly, for the normalized signal envelope ($P = R/\sqrt{\Omega}$), (17) can be re-written as follows:

$$T_P(\rho) f_m = \frac{\Gamma(m+m_s)\,\rho\left[(m_s-1)+m\rho^2\right]^{m+m_s-1}}{\Gamma\left(m+m_s-\frac{1}{2}\right)\sqrt{2m\,\pi}\,(m_s-1)^{m+m_s-\frac{1}{2}}} \times {}_2F_1\left(m+m_s, m; 1+m; -\frac{m\rho^2}{m_s-1}\right). \quad (18)$$

2) Special Cases: As in Sec. III.A, (18) can be used to derive simple and accurate approximate expressions that provide useful insights on the impact of the involved parameters on the overall system performance. To this end, when $m\rho^2 \gg m_s - 1$, it follows that $m_s - 1 + m\rho^2 \simeq m\rho^2$, which yields

$$T_P(\rho) f_m \simeq \frac{\Gamma(m+m_s) m^{m+m_s-1} \rho^{2m+2m_s-1}}{\Gamma\left(m+m_s-\frac{1}{2}\right)\sqrt{2m\pi}(m_s-1)^{m+m_s-\frac{1}{2}}} \times {}_2F_1\left(m+m_s, m; 1+m; -\frac{m\rho^2}{m_s-1}\right). \quad (19)$$

On the contrary, when $m\rho^2 \ll m_s - 1$, it follows that

$$T_P(\rho) f_m \simeq \frac{\Gamma(m+m_s)\rho\,{}_2F_1(m+m_s, m; 1+m; 0)}{\Gamma\left(m+m_s-\frac{1}{2}\right)\sqrt{2m\pi}\sqrt{m_s-1}} \quad (20)$$

which based on the identity ${}_2F_1(a,b,c,0) \triangleq 1$, reduces to

$$T_P(\rho) f_m \simeq \frac{\Gamma(m+m_s)\rho}{\Gamma\left(m+m_s-\frac{1}{2}\right)\sqrt{2m\pi(m_s-1)}}. \quad (21)$$

Finally, when $m >> m_s$, it follows that $m + m_s \approx m + 1$; now recalling the identity ${}_2F_1(a,b,a,cx) \triangleq (1-cx)^{-b}$ and after some manipulations, (18) reduces to:

$$T_P(\rho) f_m \simeq \frac{\rho(m_s-1+m\rho^2)^{m_s-1}}{\sqrt{2\pi m}(m_s-1)^{m_s-\frac{1}{2}}} \quad (22)$$

which is a simple, insightful and accurate approximation.

IV. Numerical Results

To investigate the impact of differing levels of multipath fading (m) and shadowing (m_s) upon the LCR and AFD, Fig. 1(a) and Fig. 1(b) illustrate the shape of the normalized

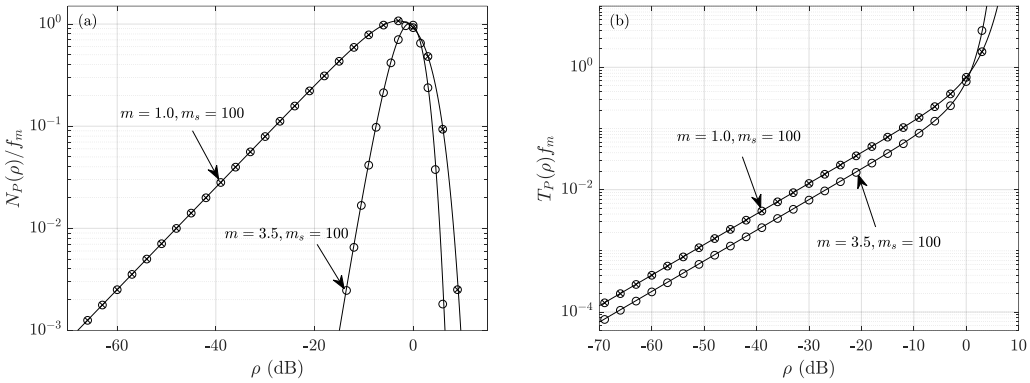

Fig. 2. Normalized (a) LCRs and (b) AFDs over $\mathcal{F}$ composite fading channels (continuous lines) for the special cases with the normalized LCRs and AFDs of the Nakagami-m (circles) and Rayleigh (x-marks) fading channels.

LCR and AFD for differing combinations of m and m_s, i.e., $m = \{1, 3, 30\}$ and $m_s = \{2, 30\}$. It is clear from Fig. 1(a) that as the multipath fading severity increases (i.e., lower values of m) and the amount of shadowing increases (i.e., lower values of m_s), the signal envelope crosses both lower and higher threshold levels more frequently. In contrast, as the severity of the multipath fading and shadowing decreases, the range of threshold levels that the signal envelope crosses is decreased. When comparing the effect of the variation of the m and m_s on the LCR, multipath fading has a more noticeable effect on the LCR compared to shadowing at lower levels. On the contrary, shadowing has a more significant effect on the LCR than multipath fading at higher levels. Furthermore, it can easily be seen from Fig. 1(b) that the signal envelope spends less time at lower fade levels and resides longer at higher threshold levels as the severity of multipath fading and shadowing conditions decreases (i.e., higher m and m_s).

When comparing the effect of the variation of the m and m_s on the AFD, shadowing has a more noticeable effect on the AFD compared to multipath fading both at lower and higher threshold levels. Interestingly, the margin between the LCR and AFD curves for light and heavy shadowing conditions increases as the multipath fading severity decreases. This suggests that the shadowing effects become more pronounced when the channel is subject to less severe multipath fading. Furthermore, the approximate LCR and AFD begin to provide good agreement with the exact LCR and AFD well before reaching the high and low threshold extremities (see Fig. 1).

It is recalled here that the $\mathcal{F}$ composite fading model becomes equivalent to the Nakagami-m fading model when there exists no shadowing (i.e., $m_s \to \infty$, although in reality a large value of m_s). Likewise, the Rayleigh fading model is deduced by setting $m = 1$ and again letting $m_s \to \infty$. Using these special cases, Fig. 2(a) and Fig. 2(b) show the normalized LCR and AFD of the $\mathcal{F}$ composite fading model coincide with those for the Nakagami-m [14, eqs. (17) and (21)] and Rayleigh [15, eqs. (4.227) and (4.228)] fading models.

V. Conclusion

Exact and approximate closed-form expressions for the LCR and AFD of the signal envelope in $\mathcal{F}$ composite fading channels have been derived. During the course of our analysis, we also obtained an expression for the joint PDF of an inverse Nakagami-m random process and its time derivative. From this expression, it has been demonstrated that the two processes are independent. Our numerical results have shown that the signal envelope crosses lower threshold levels at a lower rate, consequently spending less time at lower levels. It is also observed that as the severity of the multipath fading and shadowing decreases, the range of threshold levels that the signal envelope crosses is decreased. Finally, due to the relative simplicity of the derived expressions, they can be readily used to quantify the LCR and AFD in emergent wireless applications, such as device-to-device communications, which can be subject to simultaneous multipath and shadowing effects.

References

[1] G. C. Alexandropoulos and K. P. Peppas, "Secrecy outage analysis over correlated composite Nakagami-m/gamma fading channels," *IEEE Commun. Lett.*, vol. 22, no. 1, pp. 77–80, Jan. 2018.

[2] S. K. Yoo *et al.*, "The κ-μ / inverse gamma and η-μ / inverse gamma composite fading models: Fundamental statistics and empirical validation," *IEEE Trans. Commun.*, Dec. 2017.

[3] S. K. Yoo *et al.*, "The Fisher-Snedecor $\mathcal{F}$ distribution: A simple and accurate composite fading model," *IEEE Commun. Lett.*, vol. 21, no. 7, pp. 1661–1664, Jul. 2017.

[4] S. K. Yoo *et al.*, "A comprehensive analysis of the achievable channel capacity in $\mathcal{F}$ composite fading channels," *IEEE Access.*, vol. 7, pp. 34078–34094, Feb. 2019.

[5] J. M. Morris and J.-L. Chang, "Burst error statistics of simulated Viterbi decoded BFSK and high-rate punctured codes on fading and scintillating channels," *IEEE Trans. Commun.*, vol. 43, no. 2, pp. 695–700, Feb. 1995.

[6] J. J. Nielsen, R. Liu and P. Popovski, "Ultra-reliable low latency communication using interface diversity," *IEEE Trans. Commun.*, vol. 66, no. 3, pp. 1322–1334, Mar. 2018.

[7] P. S. Bithas, "Weibull-gamma composite distribution: alternative multipath/shadowing fading model," *Electron. Lett.*, vol. 45, no. 14, pp. 749–751, Jul. 2009.

[8] A. Abdi, W. C. Lau, M.-S. Alouini, and M. Kaveh, "A new simple model for land mobile satellite channels: First-and second-order statistics," *IEEE Trans. Wireless Commun.*, vol. 2, no. 3, pp. 519–528, 2003.

[9] S. L. Cotton, "Second-order statistics of κ-μ shadowed fading channels," *IEEE Trans. Veh. Technol.*, vol. 65, no. 10, pp. 8715–8720, Oct. 2016.

[10] F. Yilmaz and M.-S. Alouini, "A new simple model for composite fading channels: Second order statistics and channel capacity," in *Proc. ISWCS*, Sep. 2010, pp. 676–680.

[11] I. S. Gradshteyn and I. M. Ryzhik, *Table of Integrals, Series, and Products*, 7th ed. London: Academic Press, 2007.

[12] Z. Hadzi-Velkov, "Level crossing rate and average fade duration of EGC systems with cochannel interference in Rayleigh fading," *IEEE Trans. Commun.*, vol. 55, no. 11, pp. 2104−2013, Nov. 2007.

[13] F. J. Lopez-Martinez *et al.*,"Higher order statistics of sampled fading channels with applications," *IEEE Trans. Veh. Technol.*, vol. 61, no. 7, pp. 3342−3346, Sep. 2012.

[14] M. D. Yacoub, J. V. Bautista, and L. G. de Rezende Guedes, "On higher order statistics of the Nakagami-m distribution," *IEEE Trans. Veh. Technol.*, vol. 48, no. 3, pp. 790–794, May 1999.

[15] P. M. Shankar, *Fading and shadowing in wireless systems*. Springer, 2017.